Magnetic Properties of Compounds with Singlet Ground State: Exchange Correlation Effects

BERNARD R. COOPER
General Electric Research and Development Center, Schenectady, New York

(Received 10 April 1967)

Magnetic systems where the crystal-field ground state of the isolated ion is a singlet show no magnetic ordering for exchange small compared to crystal-field effects. We consider the effect of exchange as it increases from zero toward the critical value necessary for magnetic ordering with infinitesimal moment at $T=0$. In particular, we have calculated the susceptibility, nonlinear magnetization, and critical ratio of exchange to crystal-field splitting required for magnetic ordering for such systems, including exchange correlation effects by use of the constant coupling approximation. Substantial deviations from the molecular-field behavior are found at low temperatures as the exchange approaches the value required for magnetic ordering. Also we critically examine the pertinence of using boson spin-wave-like excitations to discuss thermodynamic properties in the paramagnetic case. While this formulation has certain inadequacies for treating such properties, this point of view could be quite valuable with regard to low-temperature inelastic neutron scattering experiments. Finally, the results are discussed with respect to the present experimental situation and with respect to the most promising line of investigation for future experiments.

I. INTRODUCTION

THERE is much current interest[1–12] in the magnetic properties of rare-earth compounds where the crystal-field ground state of the rare-earth ion is a singlet. For crystal-field effects, large compared to exchange, the ionic moment is completely quenched and consequently there is no magnetic ordering.[13] This situation occurs, for example, for the Tm and Pr compounds[1–9] of NaCl structure with group V anions. Such compounds have some quite interesting properties. The susceptibility at low temperatures is of a Van Vleck type brought about by the polarization of the singlet ground state. At high fields the magnetization becomes nonlinear, and the present author[4,6,7] predicted the development of a large anisotropy in the nonlinear region. This has now been observed experimentally[14,14a] in TmSb.

For compounds such as those of Tm and Pr, departures from the simple crystal-field-only susceptibility and high-field magnetization are often observed. It is a simple matter to include exchange effects on these properties within the molecular-field approximation. However, the molecular-field calculations often do not explain the observed behavior. The question then arises as to whether this lack of agreement reflects inadequacies of the molecular-field model for treating the effect of a given exchange interaction, say of a temperature-independent Heisenberg form, or whether the discrepancies must be attributed to a change of the exchange mechanism with temperature and high magnetic fields, or to some other mechanism not yet considered. This has led us to consider the question of corrections to the molecular-field behavior arising from correlation effects.

The theory obtained should also be useful in discussing experiments on magnetic systems where the exchange increases so that the threshold value for magnetic ordering is approached and exceeded. Of those rare earths having compounds of NaCl structure, Tb and Ho also have singlet crystal-field ground states; however, their compounds order magnetically. Thus, clearly, the exchange for Tb and Ho is greater than the threshold value for magnetic ordering. Then such experiments could be done on mixed rare-earth compounds with group V anions (e.g., mixed Tb-Ym or mixed Tb-Lu compounds).

Before discussing the corrections to molecular-field theory, we first consider the susceptibility for zero exchange and then the predictions of molecular-field theory. We consider the crystal-field level scheme for Tm^{3+} in an octahedral crystal field as shown in Fig. 1(a). This is the symmetry appropriate for the rare-earth compounds of NaCl structure with group V anions. This group of singlet state compounds is the most thoroughly studied at present. (The same symmetry conditions also hold for the rare-earth compounds of NaCl structure with group VI anions. Studies of singlet ground-state members of this family of

[1] H. R. Child, M. K. Wilkinson, J. W. Cable, W. C. Koehler, and E. O. Wollan, Phys. Rev. **131**, 922 (1963).
[2] D. P. Schumacher and W. E. Wallace, J. Appl. Phys. **36**, 984 (1965).
[3] G. Busch, P. Junod, F. Levy, A. Menth, and O. Vogt, Phys. Letters **14**, 264 (1965).
[4] B. R. Cooper, I. S. Jacobs, R. C. Fedder, J. S. Kouvel, and D. P. Schumacher, J. Appl. Phys. **37**, 1384 (1966).
[5] G. Busch, P. Junod, F. Levy, A. Menth, and O. Vogt, Phys. Letters **14**, 264 (1965).
[6] B. R. Cooper, Phys. Letters **22**, 24 (1966).
[7] B. R. Cooper, Phys. Letters **22**, 244 (1966).
[8] T. Tsuchida and W. E. Wallace, J. Chem. Phys. **43**, 2885 (1965).
[9] P. Junod, A. Menth, and O. Vogt, Phys. Letters **23**, 626 (1966).
[10] G. A. Smolenskii, V. P. Zhuze, V. E. Adamyan, and G. M. Loginov, Phys. Status Solidi **18**, 873 (1966).
[11] S. Kern and P. M. Raccah, J. Phys. Chem. Solids **26**, 1625 (1965).
[12] K. H. J. Buschow and J. F. Fast, Z. Physik. Chem. **50**, 1 (1966).
[13] G. T. Trammell, Phys. Rev. **131**, 932 (1963).
[14] O. Vogt (private communication).
[14a] O. Vogt and B. R. Cooper, in Proceedings of the International Congress on Magnetism, Boston, 1967 (to be published).

compounds have recently begun to be reported.[10]) However, the Van Vleck-type susceptibility is also observed in other structures such as hexagonal compounds[11] and cubic compounds of the Cu_3Au structure.[12] We choose Tm rather than Pr to treat in the numerical calculations, because for those materials investigated as yet the effects of greatest interest, the Van Vleck-type susceptibility at low temperature and the nonlinear anisotropic magnetization, for experimentally attainable fields, are much larger.

As will be discussed below, exchange correlation effects vanish with increasing temperature and magnetic field. Thus we can consider such effects quite adequately by treating a two level model, shown in Fig. 1(b), for each ion where the ground state is a Γ_1 singlet and the excited state is a Γ_4 triplet. (For the Tm group V compounds Δ, the energy splitting between the Γ_1 and Γ_4 states in zero magnetic field, is about 100°K for TmN and about 30 to 40°K for the heavier compounds.) Then the theory we develop could be used as part of an interpolation scheme for real materials. The results of the present calculation would be used at low temperature and field, while the molecular-field calculation would be used at higher temperature and field where the present calculation indicated negligible correlation effects.

For Tm^{3+} in an octahedral crystal field, the crystal-field Hamiltonian has the form[15]

$$V_c=B_4(O_4^0+5\times O_4^4)+B_6(O_6^0-21\times O_6^4). \quad (1.1)$$

Here O_4^0, O_4^4, O_6^0, and O_6^4 are specified operators for given J. So only the fourth-order constant B_4 and the sixth-order constant B_6 are necessary to completely determine V_c. It is convenient to define a parameter x in terms of the ratio B_4/B_6.

$$B_4/B_6=(x/1-|x|)[F(6)/F(4)], \quad (1.2)$$

where $F(6)$ and $F(4)$ are numerical factors specified for given J. The level scheme shown in Fig. 1 is for $x=-1$ (completely fourth-order anisotropy). As x varies, the relative splittings of the levels change, and for sufficiently great departures from $x=-1$ (for $x\gtrsim -0.55$) there are level crossings, and the Γ_1 and Γ_4 states are no longer the two lowest-lying states for Tm^{3+}. However, the physical range of interest for the rare-earth group V compounds is in the range of values of x where the Γ_1 and Γ_4 states are lowest. Moreover, since there is only one state of each of these symmetry types present, the Γ_1 and Γ_4 wave functions are independent of x. The matrix elements necessary for the present study are then available from the calculated wave functions. These are

$$\langle\Gamma_1|J_z|\Gamma_{4b}\rangle=-\tfrac{1}{2}\sqrt{2}\langle\Gamma_1|J^-|\Gamma_{4c}\rangle$$
$$=\tfrac{1}{2}\sqrt{2}\langle\Gamma_1|J^+|\Gamma_{4a}\rangle=14^{1/2}, \quad (1.3a)$$
$$\langle\Gamma_{4c}|J_z|\Gamma_{4c}\rangle=-\langle\Gamma_{4a}|J_z|\Gamma_{4a}\rangle=\tfrac{1}{2}\sqrt{2}\langle\Gamma_{4c}|J^+|\Gamma_{4b}\rangle$$
$$=\tfrac{1}{2}\sqrt{2}\langle\Gamma_{4a}|J^-|\Gamma_{4b}\rangle=\tfrac{1}{2}, \quad (1.3b)$$

Here the labels Γ_{4a}, Γ_{4b}, Γ_{4c} denote the three Γ_4 states split by a magnetic field as shown in Fig. 1(b).

It is a simple matter to find the susceptibility χ_{CF} for our model system in the absence of exchange. For each ion, the Hamiltonian is

$$\mathcal{H}=V_c-\lambda\mathfrak{B}HJ_z, \quad (1.4)$$

where λ is the Landé factor and $\mathfrak{B}$ is the Bohr magnetron. To first order in H, the eigenvalues and eigenfunctions are

$$|1\rangle=|\Gamma_1\rangle+(\lambda\mathfrak{B}H\langle\Gamma_{4b}|J_z|\Gamma_1\rangle/\Delta)|\Gamma_{4b}\rangle, \qquad E_1=0$$
$$|2\rangle=|\Gamma_{4c}\rangle, \qquad E_2=\Delta-\lambda\mathfrak{B}H\langle\Gamma_{4c}|J_z|\Gamma_{4c}\rangle$$
$$|3\rangle=|\Gamma_{4b}\rangle-(\lambda\mathfrak{B}H\langle\Gamma_{4b}|J_z|\Gamma_1\rangle/\Delta)|\Gamma_1\rangle, \qquad E_3=\Delta$$
$$|4\rangle=|\Gamma_{4a}\rangle, \qquad E_4=\Delta+\lambda\mathfrak{B}H\langle\Gamma_{4c}|J_z|\Gamma_{4c}\rangle. \quad (1.5)$$

Then

$$\chi_{CF}=\Big(\sum_{i=1}^{4}M_i\exp(-E_i/kT)\Big)/\Big(H\sum_{i=1}^{4}\exp(-E_i/kT)\Big), \quad (1.6)$$

where

$$M_i=\lambda\mathfrak{B}\langle i|J_z|i\rangle. \quad (1.7)$$

This gives

$$\chi_{CF}=[(2\lambda^2\mathfrak{B}^2\langle\Gamma_{4b}|J_z|\Gamma_1\rangle^2/\Delta)(1-\exp(-\Delta/kT))$$
$$+(2\lambda^2\mathfrak{B}^2\langle\Gamma_{4c}|J_z|\Gamma_{4c}\rangle^2/kT)\exp(-\Delta/kT)]/[1+3\exp(-\Delta/kT)]. \quad (1.8)$$

The first term gives the Van Vleck-type susceptibility at $T=0$.

Before going on to the discussion of exchange effects, it is worth avoiding one possible source of confusion with regard to (1.8). This is that the high-temperature limit of (1.8) gives an apparent nonzero paramagnetic Curie temperature,

$$1/\chi_{CF}\approx C(kT-\Theta) \quad (1.9)$$

as $T\to\infty$, where

$$C=4/(2\lambda^2\mathfrak{B}^2\langle\Gamma_{4b}|J_z|\Gamma_1\rangle^2+2\lambda^2\mathfrak{B}^2\langle\Gamma_{4c}|J_z|\Gamma_{4c}\rangle^2), \quad (1.10)$$

and

$$\Theta=\Delta\left(\frac{3}{4}-\frac{\langle\Gamma_{4b}|J_z|\Gamma_1\rangle^2+2\langle\Gamma_{4c}|J_z|\Gamma_{4c}\rangle^2}{2\langle\Gamma_{4b}|J_z|\Gamma_1\rangle^2+2\langle\Gamma_{4c}|J_z|\Gamma_{4c}\rangle^2}\right)=0.2412\Delta. \quad (1.11)$$

[15] K. R. Lea, M. J. M. Leask, and W. P. Wolf, J. Phys. Chem. Solids **23**, 1381 (1962).

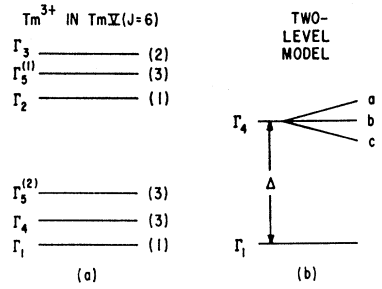

FIG. 1. (a) Level scheme for Tm^{3+} in octahedral crystal field with degeneracies of levels indicated; (b) model two-level scheme.

This apparent nonzero paramagnetic Curie temperature is an artifact of the two-level model. It would disappear if we considered all 13 levels for Tm^{3+}.

As discussed by Bleaney,[16] it is quite simple to include the effect of exchange on the susceptibility within the molecular-field approximation. With nearest-neighbor Heisenberg exchange, the Hamiltonian for the system is

$$\mathcal{H}=\sum_i (V_{ci}-\lambda\mathfrak{G}HJ_{zi})-2\mathcal{J}\sum_{\langle i,j\rangle}(\mathbf{J}_i\cdot\mathbf{J}_j), \quad (1.12)$$

where the sum over i and j is for nearest-neighbor pairs. The molecular-field approximation consists of replacing $\mathcal{H}$ by an effective Hamiltonian $\mathcal{H}_m$ for each ion.

$$\mathcal{H}_m=V_c-(\lambda\mathfrak{G}H+2\mathcal{J}z\bar{J})J_z. \quad (1.13)$$

Then

$$M=\chi_{CF}(H+2\mathcal{J}z\bar{J}/\lambda\mathfrak{G}), \quad (1.14)$$

which gives

$$1/\chi_m=H/M=1\chi_{CF}-2\mathcal{J}z/\lambda^2\mathfrak{G}^2,$$

where z is the number of nearest neighbors.

Thus the effect of exchange on the molecular-field basis is to shift the curve for $1/\chi$ for crystal-field-only rigidly down (ferromagnetic exchange) or up (antiferromagnetic exchange).

We now wish to consider correlation effects on this susceptibility behavior as well as on the high-field magnetization to be discussed in Sec. V below. The calculation we shall base most of our discussion on is of a constant coupling type.[17,18] We consider nearest-neighbor exchange, although for detailed consideration of particular materials longer range exchange will probably be present. In Sec. IV below, we also critically discuss the pertinence of boson spin-wave-like excitations in treating the paramagnetic case.

The constant coupling approximation proceeds in the following way. We first consider a single-ion Hamiltonian where the exchange effects of each neighbor are incorporated in an effective field H'.

$$\mathcal{H}_1=V_c-\lambda\mathfrak{G}(H+zH')J_z. \quad (1.16)$$

We can find a magnetization per ion for this Hamiltonian, and this magnetization, $\bar{M}_1$, will be a function of $H+zH'$. Next we consider a two-ion Hamiltonian for ions a and b, where the exchange effects of all other neighbors are given by the same effective field H'.

$$\mathcal{H}_2=V_{ca}+V_{cb}-\lambda\mathfrak{G}[H+(z-1)H'](J_{za}+J_{zb})-2\mathcal{J}\mathbf{J}_a\cdot\mathbf{J}_b. \quad (1.17)$$

Again we can find a magnetization per ion, $\bar{M}_2$, which is a function of $H+(z-1)H'$. Then the condition

$$M(H)=\bar{M}_1(H+zH')=\bar{M}_2(H+(z-1)H') \quad (1.18)$$

self-consistently determines the effective field H' and hence the magnetization. Before treating this procedure in more detail, we first point out that to first order in $\mathcal{J}/\Delta$, the susceptibility obtained from the constant-coupling calculation is identical to that from a molecular-field calculation. It is obvious that this must be so at high temperatures since the molecular-field model gives the exact result for χ to terms of order $1/T^2$, and the $1/T^2$ term giving the paramagnetic Θ is the first-order term in $\mathcal{J}$. (Thus for any magnitude of exchange the constant coupling result approaches the molecular-field result at high T.) We now show that to first order in $\mathcal{J}/\Delta$ the molecular-field and constant-coupling calculations give the same value of χ at $T=0$. The proof for general T follows along the same lines.

We regard the term $-2\mathcal{J}\mathbf{J}_a\cdot\mathbf{J}_b$ in (1.17) as a perturbation on the remainder of the Hamiltonian. Then the perturbed ground state for the two-ion system is

$$\begin{aligned}|g\rangle=|h_1,h_1\rangle&-(2\mathcal{J}\langle h_1|J_z|h_1\rangle\langle h_1|J_z|h_3\rangle/E_1-E_3)\\&\times(|h_1,h_3\rangle+|h_3,h_1\rangle)\\&-(\mathcal{J}\langle h_1|J_z|h_3\rangle^2/E_1-E_3)|h_3,h_3\rangle\\&-[\mathcal{J}\langle h_1|J^+|h_4\rangle\langle h_1|J^-|h_2\rangle/2(E_1-E_3)]\\&\times(|h_2,h_4\rangle+|h_4,h_2\rangle), \quad (1.19)\end{aligned}$$

where $|h_1\rangle$, $|h_2\rangle$, $|h_3\rangle$, $|h_4\rangle$ differ from $|1\rangle$, $|2\rangle$, $|3\rangle$, $|4\rangle$ by the replacement of H by $H+(z-1)H'$. The moment per ion at $T=0$ is given by

$$\bar{M}_{02}=\tfrac{1}{2}\lambda\mathfrak{G}\langle g|J_{za}+J_{zb}|g\rangle. \quad (1.20)$$

To first order in $\mathcal{J}$ this gives

$$\bar{M}_{02}=\lambda\mathfrak{G}\langle h_1|J_z|h_1\rangle(1-4\mathcal{J}\langle h_1|J_z|h_3\rangle^2/E_1-E_3), \quad (1.21)$$

which becomes to first order in $\mathcal{J}$ and H',

$$\bar{M}_{02}=(2\lambda^2\mathfrak{G}^2/\Delta)[H+(z-1)H']\langle\Gamma_{4b}|J_z|\Gamma_1\rangle^2+(8\lambda^2\mathfrak{G}^2H\mathcal{J}/\Delta^2)\langle\Gamma_{4b}|J_z|\Gamma_1\rangle^4. \quad (1.22)$$

[16] B. Bleaney, Proc. Roy. Soc. (London) **276A**, 19 (1963).
[17] P. W. Kasteleijn and J. P. Van Kranendonk, Physica **22**, 317 (1956).
[18] J. S. Smart, *Effective Field Theories of Magnetism* (W. B. Saunders Company, Philadelphia, 1966).

From the single ion Hamiltonian of (1.16), we obtain

$$\bar{M}_{01}=(2\lambda^2\mathcal{B}^2/\Delta)(H+zH')\langle\Gamma_{4b}\mid J_z\mid\Gamma_1\rangle^2. \quad (1.23)$$

Then the condition $\bar{M}_{01}=\bar{M}_{02}$ leads to

$$H'=(4\mathcal{J}/\Delta)\langle\Gamma_{4b}\mid J_z\mid\Gamma_1\rangle^2 H. \quad (1.24)$$

To first order in $\mathcal{J}$, this is

$$H'=2\mathcal{J}\bar{J}/\lambda\mathcal{B}. \quad (1.25)$$

However, with this expression for H', the single-ion Hamiltonian of (1.16) is the same as the molecular-field Hamiltonian of (1.13).

Thus to first order in $\mathcal{J}/\Delta$, the constant-coupling approximation gives the same susceptibility as the molecular-field approximation. This means that we can expect correlation effects to become important only as $\mathcal{J}/\Delta$ approaches the critical value necessary for magnetic ordering at $T=0$. Therefore, before proceeding to a discussion of correlation effects on the susceptibility and high-field magnetization, we first examine what changes occur for the critical value of $\mathcal{J}/\Delta$ necessary for magnetic ordering with infinitesimal moment at $T=0$ for the constant-coupling model as compared to the molecular-field model. This is done in Sec. II. In Sec. III, we discuss correlation effects on the susceptibility within the constant-coupling approximation. In Sec. IV, we critically examine the pertinence of using boson spin-wave-like excitations to discuss thermodynamic properties in the paramagnetic case. While this formulation has certain inadequacies for treating such properties, we point out that this point of view could be quite valuable with regard to low-temperature inelastic neutron scattering experiments. In Sec. V, we extend the discussion of correlation effects to the high-field region where the magnetization is nonlinear. Finally, in Sec. VI we discuss our results both with respect to the present experimental situation and with respect to the most promising line of investigation for future experiments.

II. CRITICAL VALUE OF EXCHANGE FOR MAGNETIC ORDERING

It is a simple matter to find the threshold value of $\mathcal{J}/\Delta$ necessary for ferromagnetic ordering with infinitesimal moment at $T=0$ on the molecular-field picture.[16] This is done by using the self-consistency condition for magnetic ordering at 0°K.

$$\bar{J}=\langle 1_m\mid J_z\mid 1_m\rangle, \quad (2.1)$$

where $\mid 1_m\rangle$ is the ground state of $\mathcal{H}_m$ given in (1.13) to first order in $\bar{J}$ for $H=0$.

$$\mid 1_m\rangle=\mid\Gamma_1\rangle+(2\mathcal{J}z\bar{J}\langle\Gamma_{4b}\mid J_z\mid\Gamma_1\rangle/\Delta)\mid\Gamma_{4b}\rangle. \quad (2.2)$$

This then gives the condition for ferromagnetic ordering with infinitesimal moment at $T=0$.

$$1=4z\mathcal{J}\langle\Gamma_{4b}\mid J_z\mid\Gamma_1\rangle^2/\Delta. \quad (2.3)$$

This result also could be obtained from (1.14) by requiring $1/\chi_{CF}=0$ at $T=0$. The condition for ordering with an antiferromagnetic interaction is the same as (2.3), replacing $\mathcal{J}$ by its absolute value, when the magnetic lattice is of a type where none of the nearest neighbors of a given ion are nearest neighbors of each other. (This simple situation pertains to the rare earths in the Au_3Cu structure, or if second-neighbor exchange interactions are dominant, for the NaCl lattice.)

Next we consider the critical value of $\mathcal{J}/\Delta$ with ferromagnetic exchange for the constant-coupling model. First, consider the two-ion Hamiltonian of (1.17) when $H=0$.

$$\mathcal{H}_2=\mathcal{H}_{20}+\mathcal{H}_2', \quad (2.4)$$

with

$$\mathcal{H}_{20}=V_{ca}+V_{cb}-2\mathcal{J}\mathbf{J}_a\cdot\mathbf{J}_b, \quad (2.5)$$

$$\mathcal{H}_2'=-\lambda\mathcal{B}(z-1)H'(J_{za}+J_{zb}). \quad (2.6)$$

We treat $\mathcal{H}_2'$ as a perturbation since we are interested in the case where $H'\to 0$ at $T=0$.

First we need the eigenfunctions and eigenvalues of $\mathcal{H}_{20}$ in (2.5). While to determine the critical value of $\mathcal{J}/\Delta$ necessary for magnetic ordering at $T=0$ we only need the ground-state two-ion wave functions and those wave functions mixed with the ground state by $\mathcal{H}_2'$, for later use we will need all 16 two-ion wave functions. This is made easier by noting the symmetry properties of $\mathcal{H}_{20}$. First, $\mathcal{H}_{20}$ is symmetric under interchange of ions a and b. Thus the wave functions are symmetric or antisymmetric under interchange of ions a and b. Second, $\mathcal{H}_{20}$ has Γ_1 symmetry. The two-ion crystal-field wave functions are then of three types. First is that wave function where both ions are in Γ_1 states. This wave function has Γ_1 symmetry and is symmetric in interchange of ions a and b. Second, are those wave functions with one ion in Γ_1 and the other ion in Γ_4. These two-ion states have Γ_4 symmetry and are symmetric or antisymmetric on interchange of ions a and b. Third, are those wave functions with both ions in Γ_4 states. These two-ion states have Γ_1, Γ_3, Γ_4, or Γ_5 symmetry and are symmetric or antisymmetric under interchange of ions a and b. Then $\mathcal{H}_{20}$ mixes only two-ion states that belong to the same class of the cubic group and that are both symmetric or both antisymmetric under interchange of ions a and b. Use of these properties allows us to find the 16 wave functions for $\mathcal{H}_{20}$ without dealing with any secular determinant larger than a 2×2. The 16 wave functions and energy eigenvalues for $\mathcal{H}_{20}$ are listed in the Appendix.

The ground-state wave function for $\mathcal{H}_{20}$ is

$$\mid\alpha_1\rangle=\mathfrak{N}_1\mid\Gamma_1,\Gamma_1\rangle-(\mathfrak{N}_1\nu_1/6\langle\Gamma_{4b}\mid J_z\mid\Gamma_1\rangle^2 A)\times(\mid\Gamma_{4b},\Gamma_{4b}\rangle-\mid\Gamma_{4a},\Gamma_{4c}\rangle-\mid\Gamma_{4c},\Gamma_{4a}\rangle), \quad (2.7)$$

where $\mathfrak{N}_1$ is the normalizing factor. This state has energy ν_1 where

$$\nu_1/\Delta=1+2\langle\Gamma_{4c}\mid J_z\mid\Gamma_{4c}\rangle^2 A-\tfrac{1}{2}(4+16\langle\Gamma_{4c}\mid J_z\mid\Gamma_{4c}\rangle^2 A+[16\langle\Gamma_{4c}\mid J_z\mid\Gamma_{4c}\rangle^4+48\langle\Gamma_{4b}\mid J_z\mid\Gamma_1\rangle^4]A^2)^{1/2}. \quad (2.8)$$

TABLE I. Values of $A=\mathcal{J}/\Delta$ for magnetic ordering at $T=0$.

z	6	8	12
Ferromagnetic molecular field	2.976×10^{-3}	2.232×10^{-3}	1.488×10^{-3}
Ferromagnetic constant coupling	3.663×10^{-3}	2.584×10^{-3}	1.632×10^{-3}
Antiferromagnetic molecular field	-2.976×10^{-3}	-2.232×10^{-3}	
Antiferromagnetic constant coupling	-3.654×10^{-3}	-2.579×10^{-3}	

Here we define

$$A=\mathcal{J}/\Delta. \tag{2.9}$$

The perturbation $\mathcal{H}_2'$ has Γ_4 symmetry and is symmetric in interchange of ions a and b. The function $|\alpha_1\rangle$ has Γ_1 symmetry and is symmetric in interchange of a and b. Thus $\mathcal{H}_2'$ mixes only symmetric functions under interchange of a and b of Γ_4 type with $|\alpha_1\rangle$. In particular, the only function mixed with $|\alpha_1\rangle$ is $|\alpha_4\rangle$.

$$|\alpha_4\rangle=\tfrac{1}{2}\sqrt{2}(|\Gamma_1,\Gamma_{4b}\rangle+|\Gamma_{4b},\Gamma_1\rangle \tag{2.10}$$

with energy

$$\nu_4/\Delta=1-2A\langle\Gamma_{4b}|J_z|\Gamma_1\rangle^2. \tag{2.11}$$

The ground-state function to first order in H' is

$$|\alpha_g\rangle_2=|\alpha_1\rangle -[\lambda\mathfrak{G}(z-1)H'\langle\alpha_4|J_{za}+J_{zb}|\alpha_1\rangle/(\nu_1-\nu_4)]|\alpha_4\rangle, \tag{2.12}$$

which gives the value for $\bar{J}_2$, i.e., $\bar{J}$ at $T=0$ for the two-ion Hamiltonian, as

$$\bar{J}_2=[\lambda\mathfrak{G}H'(z-1)\langle\alpha_4|J_{za}+J_{zb}|\alpha_1\rangle^2/(\nu_4-\nu_1)]. \tag{2.13}$$

The corresponding expression for the single-ion Hamiltonian of (1.16) is

$$\bar{J}_1=2\lambda\mathfrak{G}H'z\langle\Gamma_{4b}|J_z|\Gamma_1\rangle^2/\Delta. \tag{2.14}$$

Then the condition $\bar{J}_1=\bar{J}_2$ leads to the transcendental equation giving the critical value of A for ferromagnetic ordering at $T=0$

$$z/z-1=[\mathfrak{N}_1^2/(\nu_4-\nu_1)](1-(\nu_1/6\langle\Gamma_{4b}|J_z|\Gamma_1\rangle^2A))^2. \tag{2.15}$$

Solving this equation using the numerical values of metrix elements given in (1.3), gives the critical values of A shown in Table I As can be seen, the value of A necessary for magnetic ordering is significantly increased from the molecular-field-model value. Essentially, the increase can be attributed to the fact that the constant-coupling model allows for the possibility of short range as well as long-range magnetic order. This is in contrast to the molecular-field model which allows for only long-range order. As would be expected, the percentage increase in the critical value of A is greatest for the smallest number of neighbors. The percentage increase changes from just over 23% for $z=6$ to just under 10% for $z=12$.

Next we consider the critical value of A for antiferromagnetic ordering restricting ourselves to the situation where nearest neighbors of a given ion are not nearest neighbors of each other. Again we consider the two-ion Hamiltonian of (1.17) when $H=0$. Now $\mathcal{J}$ is negative. Instead of (2.6) we have

$$\mathcal{H}_2'=-\lambda\mathfrak{G}(z-1)H'(J_{za}-J_{zb}) \tag{2.16}$$

since we are looking for the value of A for which the moments of ions a and b are aligned antiparallel. Now $\mathcal{H}_2'$ is antisymmetric for interchange of a and b. Hence, $\mathcal{H}_2'$ mixes $|\alpha_1\rangle$ with $|\alpha_5\rangle$ and $|\alpha_6\rangle$ which are given in the Appendix. Then by the same sort of procedure as for the ferromagnetic case we obtain the equation determining the critical value of A in the antiferromagnetic case

$$\begin{aligned}\frac{z}{z-1}=&\frac{\mathfrak{N}_1^2\mathfrak{N}_5^2}{(\nu_5-\nu_1)}\left[1+\frac{\nu_1}{6\langle\Gamma_{4b}|J_z|\Gamma_1\rangle^2A}\right.\\&\left.+\frac{\nu_1(1+2\langle\Gamma_{4b}|J_z|\Gamma_1\rangle^2A-\nu_5)}{12\langle\Gamma_{4b}|J_z|\Gamma_1\rangle^4A^2}\right]^2\\&+\frac{\mathfrak{N}_1^2\mathfrak{N}_5^2}{(\nu_6-\nu_1)}\left[\frac{(1+2\langle\Gamma_{4b}|J_z|\Gamma_1\rangle^2A-\nu_5)}{2\langle\Gamma_{4a}|J^-|\Gamma_1\rangle\langle\Gamma_{4c}|J^+|\Gamma_{4b}\rangle A}\right.\\&\left.+\frac{\nu_1(1+2\langle\Gamma_{4b}|J_z|\Gamma_1\rangle^2A-\nu_5)}{24\langle\Gamma_{4b}|J_z|\Gamma_1\rangle^3\langle\Gamma_{4c}|J_z|\Gamma_{4c}\rangle A^2}\right.\\&\left.-\frac{\nu_1\langle\Gamma_{4c}|J_z|\Gamma_{4c}\rangle}{3\langle\Gamma_{4b}|J_z|\Gamma_1\rangle^3A}\right]^2.\end{aligned} \tag{2.17}$$

Solving this equation, using the numerical values of matrix elements given in (1.3), gives the critical values of A shown in Table I. The absolute value of the critical value of A is slightly smaller for the antiferromagnetic as compared to the ferromagnetic case in the constant-coupling approximation.

III. CORRELATION EFFECTS ON THE SUSCEPTIBILITY

From the discussion of Sec. I we expect correlation effects on the susceptibility to become important at low temperature as A approaches the critical value necessary for magnetic ordering. We now investigate this point in more detail.

First we consider the two-ion Hamiltonian of (2.4)

with $\mathcal{H}_{20}$ as given in (2.5) and

$$\mathcal{H}_2' = -\lambda\mathcal{B}[H+(z-1)H'](J_{za}+J_{zb}). \quad (3.1)$$

We should note that we use this form of $\mathcal{H}_2'$ whether the exchange is ferromagnetic or antiferromagnetic. This is because we are considering the case where the magnitude of A is below the value for magnetic ordering. Therefore, the moments of all ions are parallel even for antiferromagnetic exchange. Then it is a straightforward procedure using the unperturbed states of $\mathcal{H}_{20}$ given in the Appendix to calculate the perturbed wave functions $|\delta_i\rangle$ and energies E_i to first order in $\mathcal{H}_2'$. The magnetic moment per ion for the two-ion Hamiltonian is given to first order in $H+(z-1)H'$ by

$$\bar{M}_2 = \frac{\sum_{i=1}^{16} \tfrac{1}{2}\lambda\mathcal{B}\langle\delta_i | J_{za}+J_{zb} | \delta_i\rangle \exp(-E_i/kT)}{\sum_{i=1}^{16} \exp(-E_i/kT)}. \quad (3.2)$$

This gives $\bar{M}_2$ of the form

$$\bar{M}_2 = [H+(z-1)H']G(\Delta/T, \Delta, A). \quad (3.3)$$

Here $G(\Delta/T, \Delta, A)$ is a rather cumbersome function so we will not give the actual expression. However, as outlined above, the procedure for obtaining $G(\Delta/T, \Delta, A)$ from the eigenfunctions of $\mathcal{H}_{20}$ in the Appendix is straightforward.

On the other hand, from the single-ion Hamiltonian of (1.16) we have to first order in $H+zH'$,

$$\bar{M}_1 = (H+zH')\chi_{CF}(\Delta/T, \Delta), \quad (3.4)$$

with χ_{CF} given by (1.8). Then the condition $\bar{M}_2=\bar{M}_1$

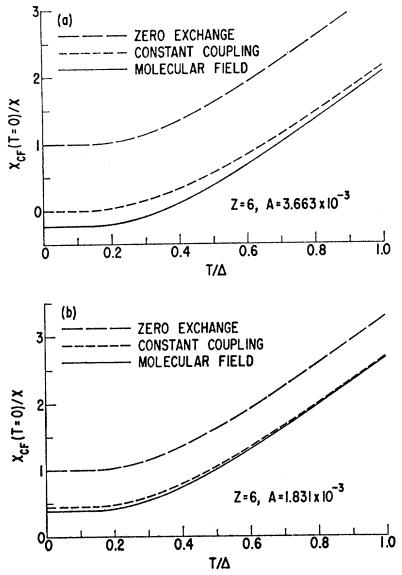

FIG. 2. (a) Inverse susceptibility versus temperature for $z=6$ and A equal to the constant-coupling ferromagnetic critical value; (b) inverse susceptibility versus temperature for A equal to half the value in (a).

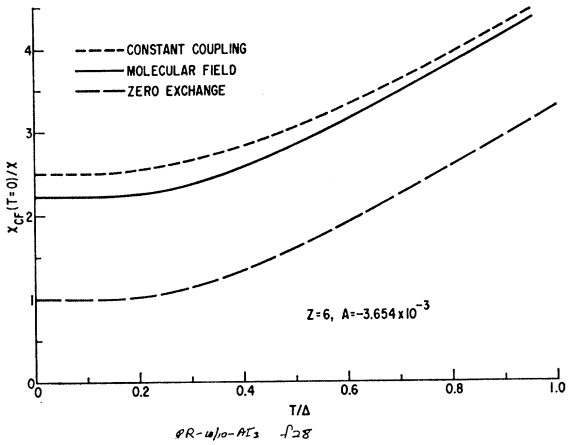

FIG. 3. Inverse susceptibility versus temperature for $z=6$ and A equal to the constant-coupling antiferromagnetic critical value.

determines

$$H' = H(G-\chi_{CF})/[z\chi_{CF}-(z-1)G]. \quad (3.5)$$

This gives the susceptibility

$$\chi = G\chi_{CF}/[z\chi_{CF}-(z-1)G]. \quad (3.6)$$

Figure 2(a) shows plots of $1/\chi$ (normalized to the crystal-field-only value at $T=0$) versus T/Δ for $z=6$ and $A=3.663\times10^{-3}$, the constant-coupling critical value for ferromagnetic ordering at $T=0$. Curves for $1/\chi$ using both the constant-coupling and molecular-field calculations for this z and A are shown as well as a curve for zero exchange. At $T=0$, the difference between the constant-coupling value of $1/\chi$ and the zero exchange value is about 19% less than the corresponding difference for the molecular-field calculation. As the number of nearest neighbors increases, continuing to take A as the critical value for ferromagnetic ordering at $T=0$, this percentage difference between constant-coupling and molecular-field shifts from the zero exchange value of $1/\chi$ at $T=0$ decreases and is about 9% for $z=12$. For given z as A decreases from the critical value, the difference between the molecular-field and constant-coupling shifts from the value of $1/\chi$ for vanishing exchange decreases more rapidly than linearly with A. (As pointed out in Sec. I, the molecular field shift of $1/\chi$ from the value for vanishing exchange is linear with A.) This is illustrated in Fig. 2(b) for $z=6$ and $A=1.831\times10^{-3}$, half the critical value. Here at $T=0$ the shift of the constant coupling $1/\chi$ from the crystal-field-only $1/\chi$ is reduced by only about 10% from the molecular-field shift for the same A.

We can also consider antiferromagnetic coupling. In Fig. 3, we plot $1/\chi$ versus Δ/T for $z=6$ and $A=-3.654$, the critical value for antiferromagnetic ordering. Here the shift of the constant coupling $1/\chi$ from the crystal-field-only $1/\chi$ is *greater* by approximately 22.4% than

the molecular-field shift. Thus the effect of correlation is to shift the curve of $1/\chi$ at low temperature upward, regardless of the sign of exchange. Correlation effects always make the plot of $1/\chi$ versus T "look flatter."

IV. SPIN-WAVE-LIKE BOSON EXCITATIONS

In this section we critically discuss the pertinence of boson spin-wave-like excitations to the magnetic behavior of induced moment systems in the paramagnetic region. Following work of Van Vleck[19] in a somewhat different context, Trammell[20,21] originally developed the idea of such spin-wave-like excitations for those rare-earth group V anion compounds where the exchange is large enough to have magnetic ordering. Grover[22] also treated the case of magnetically ordered materials, and in addition, discussed the excitation spectrum and specific heat for small exchange where the compound is paramagnetic at $T=0$. While Grover did not include effects of applied field and therefore could not discuss the magnetization in the paramagnetic region, the idea of a treatment of correlation effects on magnetization within a spin-wave-like treatment is attractive. (The difference from the usual spin-wave spectrum would be the presence of an energy gap, i.e., the spin flip occurs from the singlet ground state to a crystal-field excited level.) Unfortunately, this concept suffers from several difficulties, both conceptual and in calculational detail. However, the questions involved are sufficiently fundamental to warrant a discussion in some detail to make clear the problems. Also, on a more hopeful note, there is one very basic type of measurement for which the idea of spin-wave-like excitations is fruitful. This would be neutron inelastic scattering at low temperatures. Here even as correlation effects become important for increasing exchange, the basic dispersion behavior for the excitations would be pertinent. Indeed such observations would, among other things, give very valuable information about the range and nature of the exchange interactions.

The calculation proceeds as follows, where throughout we consider the two-level problem of Fig. 1(b). We first rewrite the Hamiltonian given in (1.12) following the procedure of Trammell and co-workers[20,21] adapted to the case at hand.

$$\mathcal{H}=\mathcal{H}_0+\mathcal{H}_1, \tag{4.1}$$

$$\mathcal{H}_0=\sum_i (V_{ci}-[\lambda\mathfrak{G}H+2\mathcal{J}(0)\langle J\rangle]J_{zi})+N\mathcal{J}(0)\langle J\rangle^2, \tag{4.2}$$

$$\mathcal{H}_1=-\sum_{i,j}\mathcal{J}_{ij}\mathbf{j}_i\cdot\mathbf{j}_j, \tag{4.3}$$

$$\mathbf{j}_i=\mathbf{J}_i-\langle J\rangle\hat{\epsilon}_z, \tag{4.4}$$

where $\hat{\epsilon}_z$ denotes a unit vector in the z direction. Here $\langle J\rangle$ is the expectation value of J_z at $T=0$ in the molecular-field approximation.

$$\langle J\rangle=[2\lambda\mathfrak{G}H\langle\Gamma_1\mid J_z\mid\Gamma_{4b}\rangle^2/\Delta(1-\eta)], \tag{4.5}$$

with

$$\eta=4\mathcal{J}(0)\langle\Gamma_1\mid J_z\mid\Gamma_{4b}\rangle^2/\Delta. \tag{4.6}$$

Then the unperturbed Hamiltonian $\mathcal{H}_0$ is the molecular-field Hamiltonian at $T=0$. The perturbation $\mathcal{H}_1$ represents the difference between the true exchange energy and the molecular-field approximation at $T=0$. Here the exchange interaction has been generalized to arbitrary range and $\mathcal{J}(0)=\sum_j\mathcal{J}_{ij}$.

The Hamiltonian of (4.1) is used to treat the magnetization at low temperature. The first stage of approximation is to replace the spin operators in (4.1) by fermion operators.

$$\mathcal{H}_0=\sum_{i,n}\epsilon_n d_{in}^{\dagger}d_{in}+N\mathcal{J}(0)\langle J\rangle^2. \tag{4.7}$$

Here $d_{in}^{\dagger}$ and d_{in} are fermion creation and annihilation operators, respectively. The fermion operators create or annihilate particles in the single-ion states;

$$\begin{aligned}
\mid g\rangle&=\mid\Gamma_1\rangle\\
&\quad+[(\lambda\mathfrak{G}H+2\mathcal{J}(0)\langle J\rangle)\langle\Gamma_1\mid J_z\mid\Gamma_{4b}\rangle/\Delta]\mid\Gamma_{4b}\rangle,\\
\mid e\rangle&=\mid\Gamma_{4b}\rangle\\
&\quad-[(\lambda\mathfrak{G}H+2\mathcal{J}(0)\langle J\rangle)\langle\Gamma_1\mid J_z\mid\Gamma_{4b}\rangle/\Delta]\mid\Gamma_1\rangle,\\
\mid c\rangle&=\mid\Gamma_{4c}\rangle,\\
\mid a\rangle&=\mid\Gamma_{4a}\rangle,
\end{aligned} \tag{4.8}$$

with energies

$$\begin{aligned}
\epsilon_g&=-[\langle\Gamma_1\mid J_z\mid\Gamma_{4b}\rangle^2(\lambda\mathfrak{G}H)^2/\Delta(1-\eta)^2],\\
\epsilon_e&=\Delta+[\langle\Gamma_1\mid J_z\mid\Gamma_{4b}\rangle^2(\lambda\mathfrak{G}H)^2/\Delta(1-\eta)^2],\\
\epsilon_a&=\Delta+\lambda\mathfrak{G}H\langle\Gamma_{4c}\mid J_z\mid\Gamma_{4c}\rangle/(1-\eta),\\
\epsilon_c&=\Delta-\lambda\mathfrak{G}H\langle\Gamma_{4c}\mid J_z\mid\Gamma_{4c}\rangle/(1-\eta).
\end{aligned} \tag{4.9}$$

The sum over n in (4.7) is then over the four single-ion states of (4.8), while i is summed over N sites in the crystal. The perturbed Hamiltonian becomes,

$$\mathcal{H}_1=-\sum_{i,j,n,m,n',m'}\mathcal{J}_{ij}\langle n\mid\mathbf{j}_i\mid m\rangle\cdot\langle n'\mid\mathbf{j}_j\mid m'\rangle d_{in}^{\dagger}d_{im}d_{jn'}^{\dagger}d_{jm'}, \tag{4.10}$$

with n, m, n', m' summed over the four single-ion states. It should be noted that the use of Fermi statistics is justified only at low temperatures. At high temperatures the fermion representation admits states with more than one of the single-ion states of (4.8) occupied for a single ion.

One then goes further with the low-temperature approximation by introducing operators

$$\begin{aligned}
a_{ie}&=d_{ig}^{\dagger}d_{ie}, & a_{ie}^{\dagger}&=d_{ie}^{\dagger}d_{ig},\\
a_{ia}&=d_{ig}^{\dagger}d_{ia}, & a_{ia}^{\dagger}&=d_{ia}^{\dagger}d_{ig},\\
a_{ic}&=d_{ig}^{\dagger}d_{ic}, & a_{ic}^{\dagger}&=d_{ic}^{\dagger}d_{ig}.
\end{aligned} \tag{4.11}$$

[19] R. M. Bozorth and J. H. Van Vleck, Phys. Rev. **118**, 1493 (1960).
[20] G. T. Trammell, J. Appl. Phys. **31**, 362*S* (1960).
[21] Y. Kitano, F. Specht, and G. T. Trammel, in *Proceedings of the International Conference on Magnetism, Nottingham* 1964 (Institute of Physics and the Physical Society, London, 1965), p. 480.
[22] B. Grover, Phys. Rev. **140**, A1944 (1965).

The commutation relationship for the $a_{in}^\dagger$ and a_{in} is

$$[a_{im}, a_{jn}^\dagger]=\delta_{ij}\delta_{nm}n_{ig}-\delta_{ij}d_{jn}^\dagger d_{im}. \quad (4.12)$$

At low temperature, $n_{ig}\approx 1$ and the second term on the right is negligible. Thus the $a_{in}^\dagger$ and a_{in} obey boson commutation relations at low temperature. We can then rewrite (4.7) and (4.10) in terms of these boson operators. Consistent with the low-temperature approximation involved in treating the a_{in} as boson operators, one takes $n_{ig}=1$ and considers only matrix elements in $\mathcal{H}_1$ involving the ground state. This gives

$$\mathcal{H}_0=N\epsilon_g+N\mathcal{J}(0)\langle J\rangle^2 + \sum_{\mathbf{q}} (\epsilon_e a_{\mathbf{q}e}^\dagger a_{\mathbf{q}e}+\epsilon_a a_{\mathbf{q}a}^\dagger a_{\mathbf{q}a}+\epsilon_c a_{\mathbf{q}c}^\dagger a_{\mathbf{q}c}), \quad (4.13)$$

where the $a_{\mathbf{q}e}$, etc., are the Fourier transforms of the a_{ie}

$$a_{ie}=N^{-1/2}\sum_{\mathbf{q}} a_{\mathbf{q}e}\exp(-i\mathbf{q}\cdot\mathbf{r}_i), \quad (4.14)$$

and

$$\mathcal{H}_1=\sum_{\mathbf{q}}\mathcal{J}(\mathbf{q})[-\langle e\mid J_z\mid g\rangle^2 \times(2a_{\mathbf{q}e}^\dagger a_{\mathbf{q}e}+a_{\mathbf{q}e}a_{-\mathbf{q}e}+a_{\mathbf{q}e}^\dagger a_{-\mathbf{q}e}^\dagger) -\langle c\mid J^+\mid g\rangle^2 a_{\mathbf{q}c}^\dagger a_{\mathbf{q}c}-\langle a\mid J^-\mid g\rangle^2 a_{\mathbf{q}a}^\dagger a_{\mathbf{q}a} -\langle c\mid J^+\mid g\rangle\langle a\mid J^-\mid g\rangle(a_{\mathbf{q}a}a_{-\mathbf{q}c}+a_{\mathbf{q}a}^\dagger a_{-\mathbf{q}c}^\dagger)]. \quad (4.15)$$

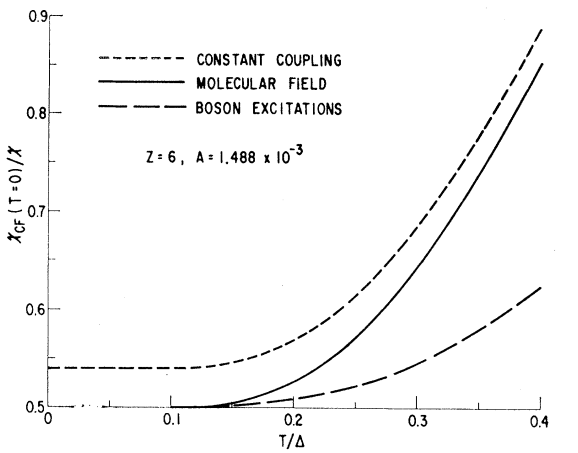

FIG. 4. Inverse susceptibility versus temperature for boson spin-wave-like calculation compared to molecular field and constant-coupling curves for same A and z.

Here $\mathcal{J}(\mathbf{q})$ is the Fourier transform of the exchange energy per ion.

$$\mathcal{J}(\mathbf{q})=\sum_i \mathcal{J}_{ij}\exp(i\mathbf{q}\cdot\mathbf{r}_{ij}). \quad (4.16)$$

The technique for diagonalizing the quadratic boson Hamiltonian is standard and gives, omitting zero-point motion terms,

$$\mathcal{H}=N(\epsilon_g+\mathcal{J}(0)\langle J\rangle^2)+\sum_{\mathbf{q}}(n_{e\mathbf{q}}E_{e\mathbf{q}}+n_{a\mathbf{q}}E_{a\mathbf{q}}+n_{c\mathbf{q}}E_{c\mathbf{q}}), \quad (4.17)$$

$$E_{e\mathbf{q}}=\Delta\left\{1-\frac{4\mathbf{J}(\mathbf{q})\langle\Gamma_{4b}\mid J_z\mid\Gamma_1\rangle^2}{\Delta}+\frac{2(\lambda\mathcal{B}H)^2\langle\Gamma_{4b}\mid J_z\mid\Gamma_1\rangle^2}{\Delta^2(1-\eta)^2}+\frac{4\mathcal{J}(\mathbf{q})(\lambda\mathcal{B}H)^2\langle\Gamma_{4b}\mid J_z\mid\Gamma_1\rangle^4}{\Delta^3(1-\eta)^2}\right\}^{1/2}, \quad (4.18)$$

$$E_{a\mathbf{q}}=\frac{\langle\Gamma_{4c}\mid J_z\mid\Gamma_{4c}\rangle\lambda\mathcal{B}H}{(1-\eta)}\left[1-\frac{4\mathcal{J}(\mathbf{q})\langle\Gamma_{4b}\mid J_z\mid\Gamma_1\rangle^2}{\Delta}\right] +\Delta\left\{\left[1-\frac{4\mathcal{J}(\mathbf{q})\langle\Gamma_{4b}\mid J_z\mid\Gamma_1\rangle^2}{\Delta}\right]\left[1-\frac{4\mathcal{J}(\mathbf{q})(\lambda\mathcal{B}H)^2\langle\Gamma_{4b}\mid J_z\mid\Gamma_1\rangle^2\langle\Gamma_{4c}\mid J_z\mid\Gamma_{4c}\rangle^2}{\Delta^3(1-\eta)^2}\right]\right\}^{1/2}, \quad (4.19)$$

$$E_{c\mathbf{q}}=-\frac{\langle\Gamma_{4c}\mid J_z\mid\Gamma_{4c}\rangle\lambda\mathcal{B}H}{(1-\eta)}\left[1-\frac{4\mathcal{J}(\mathbf{q})\langle\Gamma_{4b}\mid J_z\mid\Gamma_1\rangle^2}{\Delta}\right] +\Delta\left\{\left[1-\frac{4\mathcal{J}(\mathbf{q})\langle\Gamma_{4b}\mid J_z\mid\Gamma_1\rangle^2}{\Delta}\right]\left[1-\frac{4\mathcal{J}(\mathbf{q})(\lambda\mathcal{B}H)^2\langle\Gamma_{4b}\mid J_z\mid\Gamma_1\rangle^2\langle\Gamma_{4c}\mid J_z\mid\Gamma_{4c}\rangle^2}{\Delta^3(1-\eta)^2}\right]\right\}^{1/2}. \quad (4.20)$$

Then the $n_{e\mathbf{q}}$, $n_{a\mathbf{q}}$, $n_{c\mathbf{q}}$ are occupation-number operators for spin-wave-like states, where there is a gap from the ground state to the spin wave of lowest energy. In the ordinary ferromagnetic case, the maximum of $\mathcal{J}(\mathbf{q})$ occurs at $q=0$. Then the condition (2.3) for infinitesimal ferromagnetic ordering at $T=0$ corresponds to the condition that the $q=0$ spin wave have zero energy with $H=0$.

From the Hamiltonian of (4.17), it is a straightforward procedure to find the susceptibility

$$\chi=(kT/H)(\partial/\partial H)\{\ln\sum_n\exp(-E_n/kT)\}. \quad (4.21)$$

In (4.21) the sum is over all eigenvalues of (4.17). Then χ is given by

$$\chi=\chi_0+\chi_1+\chi_2+\chi_3, \quad (4.22)$$

where

$$\chi_0=-(N/H)(\partial/\partial H)(\epsilon_g+\mathcal{J}(0)\langle J\rangle^2)=[2N\langle\Gamma_{4b}\mid J_z\mid\Gamma_1\rangle^2\lambda^2\mathfrak{B}^2/\Delta(1-\eta)] \tag{4.23}$$

$$\chi_1=-\frac{V}{(2\pi)^3}\sum_{n=1}^{\infty}\int_{\mathrm{BZ}}d\mathbf{q}\left[H^{-1}\frac{\partial E_{eq}}{\partial H}\exp\left(\frac{-nE_{eq}}{kT}\right)\right], \tag{4.24}$$

$$\chi_2=-\frac{V}{(2\pi)^3}\sum_{n=1}^{\infty}\int_{\mathrm{BZ}}d\mathbf{q}\left\{H^{-1}\frac{\partial(E_{aq}+E_{cq})}{\partial H}\exp\left[\frac{-n(E_{aq}+E_{cq})}{2kT}\right]\right\}, \tag{4.25}$$

$$\chi_3=-\frac{V}{(2\pi)^3}\sum_{n=1}^{\infty}\int_{\mathrm{BZ}}d\mathbf{q}\left\{H^{-1}\frac{\partial E_{3q}}{\partial H}\exp\left(\frac{-nE_{3q}}{kT}\right)+H^{-1}\frac{\partial E_{4q}}{\partial H}\exp\left(\frac{-nE_{4q}}{kT}\right)\right\}, \tag{4.26}$$

$$E_{3q}=[\langle\Gamma_{4c}\mid J_z\mid\Gamma_{4c}\rangle\lambda\mathfrak{B}H/(1-\eta)](1-(4\mathcal{J}(\mathbf{q})\langle\Gamma_1\mid J_z\mid\Gamma_{4b}\rangle^2/\Delta))+\Delta(1-(4\mathcal{J}(\mathbf{q})\langle\Gamma_1\mid J_z\mid\Gamma_{4b}\rangle^2/\Delta))^{1/2}, \tag{4.27a}$$

$$E_{4q}=-[\langle\Gamma_{4c}\mid J_z\mid\Gamma_{4c}\rangle\lambda\mathfrak{B}H/(1-\eta)](1-(4\mathcal{J}(\mathbf{q})\langle\Gamma_1\mid J_z\mid\Gamma_{4b}\rangle^2/\Delta))+\Delta(1-(4\mathcal{J}(\mathbf{q})\langle\Gamma_1\mid J_z\mid\Gamma_{4b}\rangle^2/\Delta))^{1/2}. \tag{4.27b}$$

Here χ_1, χ_2, and χ_3 are evaluated in the limit $H\to 0$. Note that the integral over $\mathbf{q}$ in (4.24), (4.25), and (4.26) is restricted to the first Brillouin zone.

In the numerical calculations, we evaluate the integral over the first Brillouin zone of the fcc lattice by using the common practice[23] of evaluating the integrand at 2048 values of $\mathbf{q}$ in the Brillouin zone (actually 89 distinct points properly weighted for $\frac{1}{48}$ of the Brillouin zone). Then

$$\frac{V}{(2\pi)^3}\int_{\mathrm{BZ}}d\mathbf{q}F(\mathbf{q})=\frac{N}{2048}\sum_{\mathbf{q}i}F(\mathbf{q}_i), \tag{4.28}$$

with $\mathbf{q}_i$ summed over the 2048 values distributed within the Brillouin zone.

Before proceeding further we should note, putting aside the question of the conceptual correctness of the present treatment for $T>0$, that spurious results will be obtained for various thermodynamic properties if the sum over $\mathbf{q}$ is not restricted properly to the first Brillouin zone. In particular, Grover following Bozorth and Van Vleck finds an enhanced specific heat C_v in the paramagnetic region. However, the enhancement occurs only because Grover uses the long wavelength expansion for $\mathcal{J}(q)$, i.e., $\mathbf{J}(q)\approx Cq^2$ and extends the integral over q out to ∞. Referring to Bozorth and Van Vleck, one sees that the proposed enhancement occurs because the effective number of nearest neighbors

$$z_{\mathrm{eff}}=6\sum_j\mathcal{J}_{ij}/\sum_j(r_{ij}/l)^2\mathcal{J}_{ij} \tag{4.29}$$

is quite large, 30 or so. This occurs if the curve of $\mathcal{J}(\mathbf{q})$ is quite flat, i.e., initially almost constant for substantial values of $\mathbf{q}$ as occurs with a long-range Rudermann-Kittel exchange interaction. However, when this is the case, it turns out that the contribution that leads to great enhancement of C_v or χ over the values appropriate to uncoupled ions comes from integration over values of q outside the first Brillouin zone.

Returning to the evaluation of χ given by Eqs. (4.22) through (4.27), this proceeds in a straightforward way using the summation indicated in (4.28) and the usual summation over n for boson statistics;

$$\sum_{n=1}^{\infty}e^{-nx}=(e^x-1)^{-1}. \tag{4.30}$$

In Fig. 4, we show the inverse susceptibility calculated for the boson model. Here we have taken an fcc lattice with second-nearest-neighbor exchange only. Thus $z=6$. The magnitude of the exchange constant has been chosen so A is half the critical value for infinitesimal ferromagnetic ordering at $T=0$ in the molecular-field approximation. The corresponding curves for the same z and A are also shown in the molecular field and constant-coupling approximations. We see that the boson excitation value for $1/\chi$ is the same as the molecular-field value at $T=0$, but does not rise as sharply for increasing T. Matching the molecular-field curve at $T=0$ is "built into" the boson calculation. This is because at $T=0$, the energy is given by $\mathfrak{IC}_0$ of (4.2) which is just the molecular-field Hamiltonian. As discussed in Sec. I, correlation effects giving departures from the molecular-field behavior come from contributions greater than first order in $\mathcal{J}/\Delta$. Such contributions come from the effect of $\mathfrak{IC}_1$ of (4.3) in the boson treatment. Since the effects of $\mathfrak{IC}_1$ come into play only as the spin-wave states become occupied, correlation effects enter only as T departs from zero. This is why the boson curve for $1/\chi$ is flatter than the molecular-field curve. The effects of $\mathfrak{IC}_1$ are higher than first order in $\mathcal{J}/\Delta$ because $\mathfrak{IC}_1$ is treated as a diagonal perturbation on $\mathfrak{IC}_0$ which is already first order in $\mathcal{J}$. It is very difficult to attach any detailed meaning to the behavior of $1/\chi$ for increasing T in the boson approximation since all the approximations involved in this calculation break down as the excited states become occupied. Numerically, the largest effect causing $1/\chi$ to remain flat as temperature increases to a significant fraction of Δ is the neglect of the depopulation of the singlet-ion ground-state implicit in the boson treatment. As already remarked above, the constant-coupling curve for $1/\chi$ approaches the molecular-field

[23] G. A. Burdick, Phys. Rev. **129**, 138 (1963).

curve at high T and is thus "flatter" than the molecular-field curve. The boson treatment indicates that a more exact treatment may show the "flattening" becoming significant at lower temperatures than given by the constant-coupling approximation.

To summarize, the bosonlike treatment suffers from two fundamental difficulties in treating situations where $\mathcal{J}/\Delta$ is smaller than the critical value necessary for infinitesimal magnetic ordering at $T=0$. First, it includes only first-order effects in $\mathcal{J}/\Delta$ at $T=0$ and therefore does not include correlation effects at $T=0$. Second, for increasing T the various approximations involved break down so that $1/\chi$ does not approach the molecular-field value at very high T. We should point out that the first objection loses its significance as $\mathcal{J}/\Delta$ increases and one obtains large ordered moment at $T=0$. In this ultimate limit of very large exchange, the boson treatment becomes the usual spin-wave treatment which treats the correlation effects correctly at low T. Also, various interpolation schemes such as the random phase approximation (RPA) Green's function method can be used to go to the high T molecular field limit in that case. On the other hand, we know that as crystal-field effects become insignificant the constant coupling approximation does not give the correct answer at $T=0$ for the Heisenberg ferromagnet, i.e., the moment per ion is slightly less than that for full alignment. Clearly, the most difficult region to treat is that for $\mathcal{J}/\Delta$ substantially greater than the value for ordering, but where $\mathcal{J}/\Delta$ is still too small to give values of ordered moment at $T=0$ close to the free ion value. The difficulty for the induced ferromagnet (or induced antiferromagnet) problem as opposed to the usual ferromagnetism by alignment of ionic moments is that the ground state and its moment are not intuitively evident. In this respect the induced ferromagnetism problem is more like the ordinary Néel antiferromagnetism than like ordinary ferromagnetism by alignment.

As already indicated above, while the boson approximation is inadequate for calculating thermodynamic properties in the paramagnetic region where $\mathcal{J}/\Delta$ is less than the critical value, the dispersion law of (4.17) should still be quite fruitful for low-temperature neutron inelastic-scattering studies. Such studies would be quite informative on the range of exchange interactions present. There is also the interesting possibility of doing low-temperature inelastic-neutron-scattering experiments on mixed Tb-Y or Tb-Lu compounds with group V anions. One could vary the composition to go toward the critical value of exchange for magnetic ordering. One could watch the change in nature of the excitation spectrum as the energy gap decreased and as correlation effects became important.

The most hopeful way of correcting the inadequacies of the quasiexcitation treatment would be to return to the fermion formulation of (4.7) and (4.10). Clearly, if one could solve the fermion Hamiltonian exactly, the breakdown of Fermi statistics at higher T would present no great problem. In calculating thermodynamic properties, one could restrict traces to exclude unphysical states. Unfortunately, this does not represent a practical program. However, for the two-level problem, i.e., excited state a singlet rather than a triplet, one might be able to include much of the correlation effects using an equation-of-motion technique. (In practice, this would apply, say, for Pr^{3+} in a hexagonal environment as in PrF_3. For the two-level system, the constraint that one is either in one state or the other at a given site limits one to one fermion creation and annihilation operator per site.) The lowest-order equation of motion would involve terms in three fermion operators, coming from the commutator of a fermion operator with $\mathcal{H}_1$. Truncation at that stage by reducing the equation to one linear in fermion operators by replacing products of two fermion operators by expectation values would presumably give the molecular-field approximation. However, proceeding to the next highest-order equation of motion before truncating would include some correlation effects. It is not clear whether this would represent a tractable calculational program.[24]

Note added in proof. Y. L. Wang and B. R. Cooper have now succeeded in treating the two-singlet-level problem using a pseudospin formalism. Applying the techniques which are familiar in standard spin problems, an improved collective excitation spectrum is found with a gap which decreases as the exchange increases. The critical strength of exchange interaction necessary for ferromagnetic ordering at $T=0$ is greater than that obtained from molecular field theory, but is close to the value calculated by the constant-coupling approximation.

V. CORRELATION EFFECTS ON THE HIGH-FIELD MAGNETIZATION

It is clear that for increasing magnetic fields the magnetization cannot increase linearly with applied field indefinitely. For the Tm^{3+} ion, the magnetization evantually saturates at 7 Bohr magnetons per ion; while for the two-level model the magnetization saturates at $\lambda\langle\Gamma_1 \mid J_z \mid \Gamma_{4b}\rangle=4.365$ Bohr magnetons per ion. As has been pointed out by the present author[4,6,7] and observed experimentally,[14,14a] the magnetization is anisotropic in the nonlinear region. However, our two-level model does not include such anisotropic effects. At 0°K the anisotropy for the complete Tm^{3+} level scheme occurs, because in the nonlinear magnetization regime, for the $\langle 111\rangle$ direction the $\Gamma_5^{(2)}$ state is significantly mixed into the Γ_1 ground state. For the $\langle 100\rangle$ direction there is no such mixing. Thus, by neglecting the presence of higher excited states, we eliminate consideration of anisotropy effects. Actually, the two-level calculational does give a very good approximation to

[24] We have had an interesting discussion of these possibilities with Dr. Y.-L. Wang.

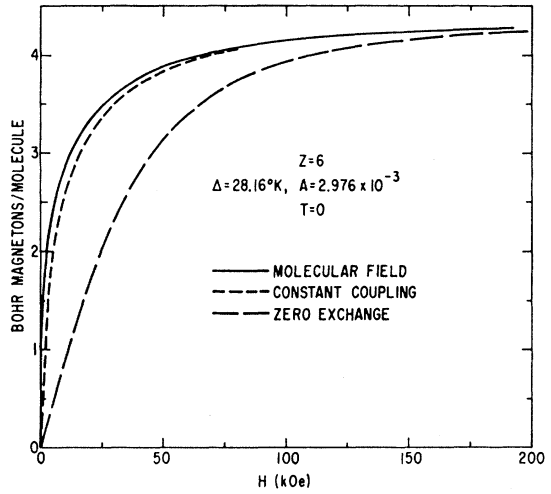

FIG. 5. Constant-coupling magnetization versus applied field at $T=0$ compared to molecular-field magnetization for A equal to the molecular-field ferromagnetic critical value.

the $\langle 100\rangle$ magnetization at low temperatures for the complete Tm^{3+} level scheme as shown in Fig. 1 for an appreciable range of magnetic field. The departure comes only at quite high fields where the first excited state crosses the ground state. For such high fields correlation effects are quite small. Thus, in the crossing region, a molecular-field treatment is adequate.

Before including exchange effects, we first consider the high-field magnetization when only crystal-field effects are present. To find the magnetization for all values of H involves diagonalizing the Hamiltonian of (1.4). This is quite simple since the only states that mix are $|\Gamma_1\rangle$ and $|\Gamma_{4b}\rangle$. Then the magnetization is given by

$$M_{CF}=[\sum_{i=1}^{4} M_i \exp(-E_i/kT)]/[\sum_{i=1}^{4} \exp(-E_i/kT)], \tag{5.1}$$

where M_i is defined in (1.7). The only change is that $|1\rangle$ and $|3\rangle$ differ from the expressions in (1.5) by using the exact expressions to all orders in H. Typical behavior for the magnetization so obtained is shown in Fig. 5 for $T=0$. (As a typical value for the numerical calculations of this section we use Δ appropriate to TmSb.)

It is also a simple matter to include exchange effects within the molecular-field approximation. This is most easily done by regarding the crystal-field-only magnetization curve shown in Fig. 5 as a plot of magnetization versus H_{eff} with

$$H_{\text{eff}}=H+(2\mathcal{J}zM/\lambda^2\mathcal{G}^2). \tag{5.2}$$

Then for specified $\mathcal{J}$ and z, for each value of M on the crystal-field-only curve, the applied field H is obtained from (5.2) by regarding the abscissa in Fig. 5 as H_{eff}. For $z=6$ and $\mathcal{J}$ equal to the critical value for ferromagnetic ordering with infinitesimal moment at $T=0$ for the molecular-field model, the molecular-field magnetization is as shown in Fig. 5.

Now we wish to consider exchange correlation effects on the magnetization within the constant-coupling approximation. First, we must find the magnetization, $\bar{M}_1$, corresponding to the single-ion Hamiltonian of (1.16) as a function of $H+zH'$. This is given by the crystal-field-only magnetization curve as in Fig. 5 where now the abscissa is $H+zH'$ rather than H. This gives the value of $\bar{M}_1$, for any value of H_1, where

$$H_1=H+zH'. \tag{5.3}$$

Next, we must calculate the magnetization $\bar{M}_2$ for the two-ion Hamiltonian of (1.17). This requires solving for the 16 exact eigenfunctions and eigenvalues of $\mathcal{H}_2$. The largest secular determinant that must be solved is a 4×4. In particular, there is one 4×4 secular determinant (mixing $|\alpha_1\rangle$, $|\alpha_2\rangle$, $|\alpha_3\rangle$, and $|\alpha_4\rangle$ given in the Appendix), five 2×2 determinants (mixing $|\alpha_5\rangle$ and $|\alpha_6\rangle$, $|\alpha_7\rangle$ and $|\alpha_8\rangle$, $|\alpha_9\rangle$ and $|\alpha_{10}\rangle$, $|\alpha_{12}$ and $|\alpha_{13}\rangle$, $|\alpha_{14}\rangle$ and $|\alpha_{15}\rangle$), and two 1×1 determinants ($|\alpha_{11}\rangle$ and $|\alpha_{16}\rangle$).

Then the magnetization $\bar{M}_2$ can be found for any value of H_2 with

$$H_2=H+(z-1)H' \tag{5.4}$$

from expression (3.2) where now $|\delta_i\rangle$ and E_i are the exact eigenfunctions and eigenvalues of $\mathcal{H}_2$ to all orders in H_2.

Thus we have two curves available, $\bar{M}_1(H_1)$, and $\bar{M}_2(H_2)$. For any particular value of magnetization M from $\bar{M}_1=M$, H_1 is equal to some value C_1; and from $\bar{M}_2=M$, H_2 is equal to some value C_2. Then the value of H' and of H for that value of magnetization are given by

$$H'=C_1-C_2, \tag{5.5a}$$

$$H=C_1(1-z)+zC_2. \tag{5.5b}$$

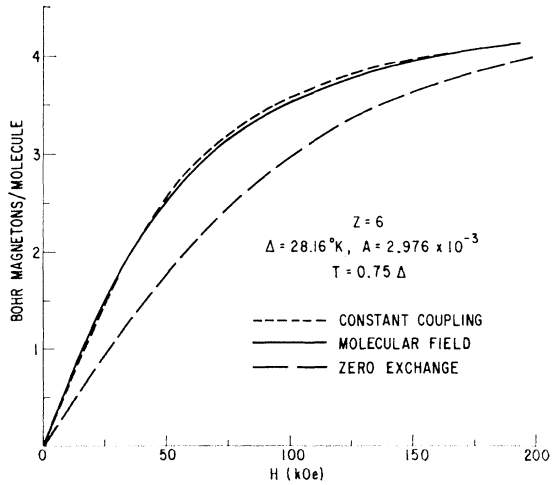

FIG. 6. Constant-coupling magnetization versus applied field at $T=0.75\Delta$ compared to molecular-field magnetization for A equal to the molecular-field ferromagnetic critical value.

Specification of H for each value of M then gives the curve for variation of magnetization with applied field H.

A magnetization curve obtained in this way at $T=0$ is also shown in Fig. 5 for the molecular-field critical value of A for $z=6$. (By restricting A to the molecular-field critical value or less, we avoid confusion from having to deal with any ordered state for any of the magnetization curves.) In the linear region the magnetization is, of course, shifted downward with respect to the molecular-field curve by the same percentage as the susceptibility discussed in Sec. III. As the magnetization approaches saturation, the difference between the molecular-field and constant-coupling magnetization becomes negligible. For increasing temperature, the correlation effects become more complex. This is illustrated in Fig. 6 for the same parameters as Fig. 5 with $T=0.75\Delta$. Here, for increasing field, the constant-coupling magnetization crosses the molecular-field-magnetization curve. Increasing complexity of correlation effects also occurs in the behavior for decreasing exchange. Figure 7(a) shows the magnetization at $T=0$ for ferromagnetic exchange decreased, by about 40% from the value in Fig. 7, to half the constant-coupling critical value. As follows from the susceptibility behavior, the effect of decreasing the exchange is to decrease the difference between the molecular-field magnetization and the constant-coupling magnetization more than proportionately. The effect of increasing temperature is shown in Fig. 7(b) for $T=0.75\Delta$. Here the constant-coupling curve crosses the molecular-field curve at relatively low field. At intermediate field values the correlation effects, while still small, are more important than at $T=0$.

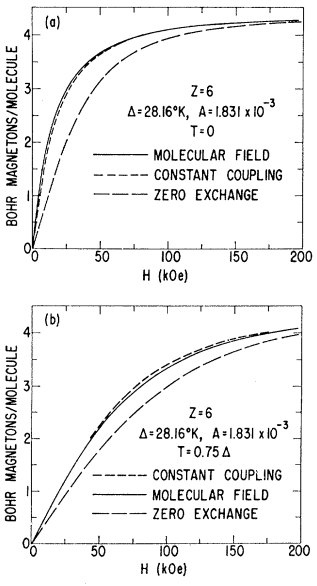

FIG. 7. (a) Magnetization versus applied field at $T=0$ for A equal to half the constant-coupling ferromagnetic critical value; (b) Magnetization for same parameters as (a) for $T=0.75\Delta$.

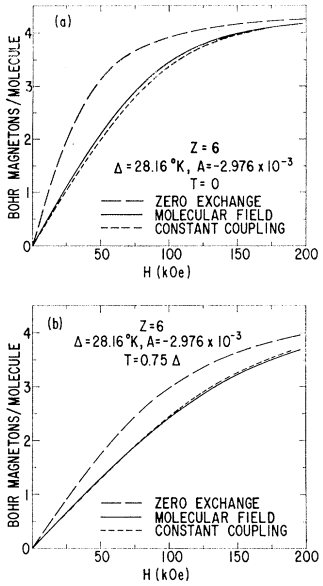

FIG. 8. (a) Magnetization versus applied field at $T=0$ for A equal to the molecular-field antiferromagnetic critical value; (b) magnetization for same parameters as (a) for $T=0.75\Delta$.

The effect of correlation on the high-field magnetization with antiferromagnetic exchange is illustrated in Fig. 8. Here A has the molecular-field critical value for antiferromagnetic ordering with infinitesimal moment at $T=0$. Just as for the corresponding ferromagnetic case at $T=0$, the constant-coupling magnetization curve falls below the molecular-field curve. As shown in Fig. 8(b), for increasing temperature the correlation effects become quite small, and the constant-coupling curve crosses the molecular-field curve to lie slightly higher for increasing field.

VI. DISCUSSION, EXPERIMENTAL SITUATION

Comparison of the results of the preceding sections with the currently available experimental data suffers from one great difficulty. This is that our discussion has proceeded on the basis that the values of crystal field and exchange parameters are available independent of the magnetization measurements. In fact, for most of the materials studied as yet, data determining these parameters independent of the susceptibility data are not available. If such is the case, one is typically faced with the following situation. If the data for $1/\chi$ extend to sufficiently high temperature, one deduces the exchange parameter from the presence of Curie-Weiss behavior. This then leaves the determination of the two crystal-field parameters,[15] x specifying the ratio of fourth- to sixth-order anisotropy, and W giving the absolute scaling of the crystal-field level scheme. Usually the magnetization is sufficiently insensitive to x so that one can choose a reasonable value for that parameter. For example, for the Tm group V anion compounds any choice of x between -0.6 and -1 gives much the

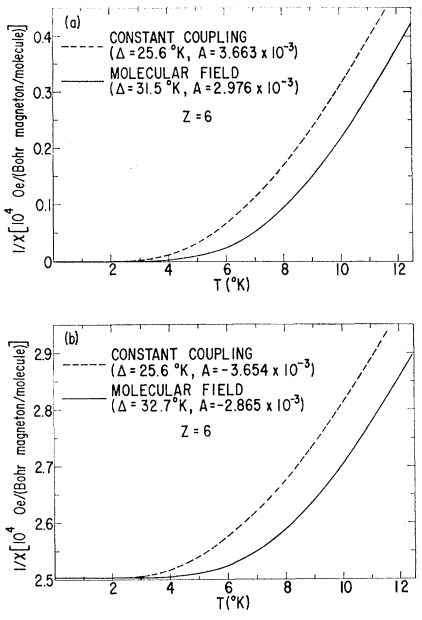

FIG. 9. (a) Inverse susceptiblity versus temperature for constant-coupling and molecular-field calculations for same $\mathcal{J}$ with $1/\chi$ matched at $T=0$; (b) Same as (a) for antiferromagnetic exchange.

same susceptibility behavior[6] once the susceptibility is fixed at $T=0$. Then the value of $1/\chi$ at $T=0$ is used to determine W. This means that to compare the susceptibility including correlation effects to the molecular-field value involves a situation such as that shown in Fig. 9. In Fig. 9(a) we have chosen a situation with ferromagnetic exchange where $1/\chi$ equals zero at $T=0$, i.e., the critical condition for infinitesimal ferromagnetic ordering. We take the same value of exchange constant for both the molecular-field and constant-coupling calculations. Then the high-temperature susceptibility is also the same for both cases. To match $1/\chi$ both at $T=0$ and at high temperature involves taking a larger value of Δ for the molecular-field case. (As a convenient scale for typical values of Δ, we choose Δ in the constant-coupling case to give $1/\chi=10^4$ Oe/Bohr magnetions per molecule for vanishing exchange.) Doing this, the molecular-field curve for $1/\chi$ is flatter than the constant-coupling curve for low T. This is in distinction to the situation discussed earlier (see Fig. 2) where for the same Δ and J the constant-coupling curve for $1/\chi$ has smaller change in going from low to high T. This contrast comes about because for the same Δ, as shown in Fig. 2, the approach of the constant-coupling curve for $1/\chi$ to the molecular-field curve occurs for T appreciable compared to Δ. In matching $1/\chi$ at $T=0$ for both constant-coupling and molecular-field curves one gets different Δ's. At low temperatures the flattening effect of correlation on $1/\chi$ is not enough to compensate for the decreased Δ in the constant-coupling case, so one gets the situation shown in Fig. 9(a). For the antiferromagnetic case shown in Fig. 9(b) taking $\mathcal{J}$ the same and matching $1/\chi$ at $T=0$ also gives a flatter curve in the molecular-field case. (Here $\mathcal{J}$ has been chosen as the constant-coupling critical value for infinitesimal antiferromagnetic ordering at $T=0$.)

The difficulty in using this procedure (matching $1/\chi$ at $T=0$ and at very high T for determining exchange and crystal-field parameters) in practice is that the shift in $1/\chi$ involved in going from the zero-exchange case to the case of infinitesimal ordered moment at $T=0$ is quite small compared to the high-temperature values of $1/\chi$. For the antiferromagnetic case for example, if the exchange is near the critical value, this shift is approximately half the value of $1/\chi$ at $T=0$. In this connection, it is worth pointing out that for a given $1/\chi$ at $T=0$, Δ for antiferromagnetic exchange is smaller than that for zero exchange which in turn is smaller than that for ferromagnetic exchange. Thus matching $1/\chi$ at $T=0$, one obtains the fastest increase of $1/\chi$ with T for antiferromagnetic exchange, and the slowest for ferromagnetic exchange.

The largest body of magnetic measurements currently available for singlet–ground-state systems is on the rare-earth compounds of NaCl structure with group V anions. In particular, the Pr and Tm compounds do not order magnetically and show Van Vleck type susceptibilities at low temperature. Matching $1/\chi$ at $T=0$ for their PrN measurements, Schumacher and Wallace[2] obtain a zero-exchange theoretical curve falling off more slowly than experiment. Following the same procedure for PrP and PrAs, Tsuchida and Wallace[8] get the reverse result, zero-exchange theory for $1/\chi$ falling off more rapidly than experiment. Since one expects any exchange to be ferromagnetic for PrN and antiferromagnetic for PrP and PrAs, as discussed in the preceding paragraph this behavior is opposite to any effect expected for exchange. Actually, at the moment the experimental situation for the Pr compounds is not very well defined. For PrN, Busch *et al.*[3] get values of $1/\chi$ at low T quite different from those of Schumacher and Wallace. Junod *et al.*[9] have also done susceptibility measurements for PrP and PrAs. They do not present their data, but do say that they get good agreement with crystal-field-only calculations of $1/\chi$.

The Tm compounds TmP, TmAs, TmSb experimentally[5] all give slightly flatter $1/\chi$ curves than are explained by a crystal-field-only calculation[6] matching $1/\chi$ at $T=0$. Again, if exchange is antiferromagnetic, this is the wrong direction for discrepancies in $1/\chi$ between crystal-field-only theory and experiment caused by exchange effects. In any case, the discrepancies are rather small, especially for TmSb, and the published data of Busch *et al.* give no evidence of Curie-Weiss behavior. For both the Tm and Pr compounds, as already indicated above, the difference between a Curie law and a Curie-Weiss law for $1/\chi$ for exchange close to the critical value would be small. A most careful

examination of the high-temperature $1/\chi$ would be warranted in light of the present discussion. It would be even better to have independent determinations of the exchange and crystal-field parameters.

There are a number of types of experiments that would independently help to determine the crystal-field and exchange parameters. Among these are specific heat measurements, inelastic neutron paramagnetic scattering, nuclear magnetic resonance, far infrared optical absorption, and fluorescence experiments on dilute magnetic systems.

One of the most promising such experiments is paramagnetic resonance[4,25,26] on one of the excited triplet states. As yet this experiment has been performed and analyzed only for TmN. As described below, the magnetization behavior for TmN is anomalous. It is possible that this arises from chemical difficulties, or there may be some more fundamental reason. In any case, the rare-earth nitrides are much more chemically unstable than the heavier compounds, and this makes them more difficult to deal with experimentally. Actually, of the Tm compounds, the most promising for resonance studies is probably TmP. This is much more stable chemically than TmN. Also TmP is not so metallic as the heavier compounds, and this makes resonance experiments more practical.

For the sake of completeness, we here give the results expected for TmN for the susceptibility and high-field magnetization using the crystal-field and exchange parameters obtained from paramagnetic resonance. (In comparing theory and experiment, it should be borne in mind that the experimental susceptibility at $T=0$ was used in conjunction with the resonance data to determine the parameters.) The values of the crystal-field parameters from resonance[26] are $x=-0.990$, $W=-3.47$°K. The exchange is given by $\mathcal{J}(0)J(J+1)=11.4$°K. (This exchange is ferromagnetic, and therefore the possibility of antiferromagnetic exchange previously considered is eliminated.) For the molecular-field model, this exchange is only about 15% of the value necessary for ferromagnetic ordering with infinitesimal moment at $T=0$. Since the exchange is so much less than the critical value for ferromagnetic ordering at $T=0$, the molecular-field approximation should be quite adequate for calculating the susceptibility and high-field magnetization.

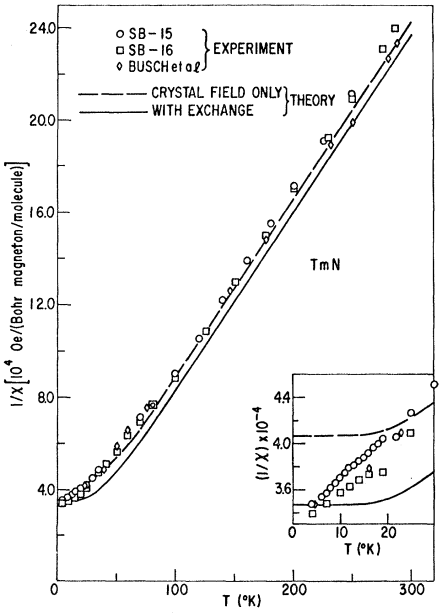

FIG. 10. Inverse susceptibility versus temperature for TmN.

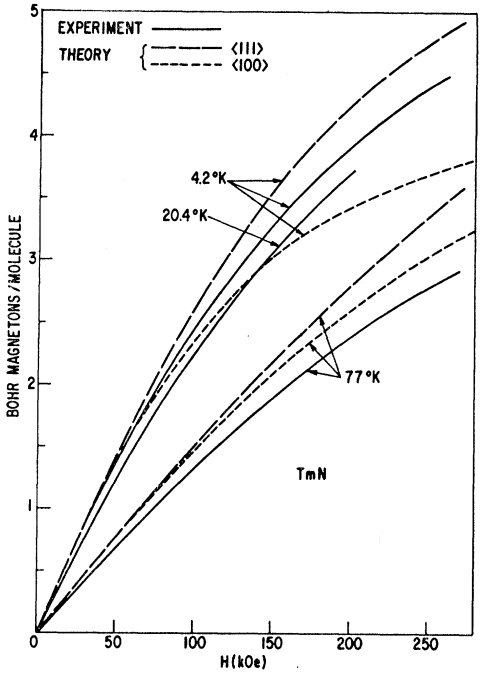

FIG. 11. Magnetization versus applied field for TmN.

The molecular-field susceptibility is shown in Fig. 10 compared to experiment.[3,4] The experimental behavior is quite anomalous. The experimental results actually give good agreement with the theory for vanishing exchange down to about 20°K. Then the curve for $1/\chi$ has a kink and continues downward for samples SB-15 and SB-16 made by Schumacher. The measurements of Busch *et al.* for $1/\chi$ also continue downward below 20°K, perhaps without a kink. If the anomalous behavior is a chemical effect, it is larger than would be anticipated for the method of preparation used.[27] The comparison of high-pulsed-field magnetization experiments[4] with theory as shown in Fig. 11 does not clarify the situation. Here the sample was a powder. Under

[25] R. C. Fedder, B. R. Cooper, and D. P. Schumacher, Bull. Am. Phys. Soc. 11, 15 (1966).
[26] B. R. Cooper, R. C. Fedder, and D. P. Schumacher (to be published).
[27] D. P. Schmacher (private communication).

appropriate conditions, a polycrystalline sample gives the easy axis magnetization for high pulsed fields. This was seen from the measurements on TmP, TmAs, and TmSb. However, it is not completely certain that the TmN sample would give the easy axis magnetization under the experimental conditions used. This may account for some of the discrepancy between experiment and the theoretical easy axis magnetization. More puzzling is the difference between experiment at 4.2 and 20.4°K. Theory would indicate a negligible difference in magnetization between these two temperatures.

While the puzzling behavior of TmN is quite interesting, a detailed study of the heavier Tm compounds of NaCl structure with group V anions is much more promising because of their greater chemical stability and ease of preparation. For TmSb a very detailed experimental study on single crystals is currently in progress and will be reported separately together with the pertinent theory. More generally, it would seem that the most promising line of approach to examining the importance of correlation effects as exchange approaches and exceeds the critical value for infinitesimal magnetic ordering at $T=0$ is to work with mixed rare-earth crystals. Tb^{3+} also has $J=6$, and hence has the same crystal-field symmetry properties as Tm^{3+}. The Tb compounds order magnetically. Thus mixed Tb-Y or Tb-Lu antimonides would seem to be a very promising material for investigation.

ACKNOWLEDGMENT

The author is grateful to E. Krieger for her able assistance with the numerical calculations.

APPENDIX

$$\mathcal{H}_{20}=V_{ca}+V_{cb}-2\mathcal{J}\mathbf{J}_a\cdot\mathbf{J}_b \tag{A1}$$

We define

$$A\equiv\mathcal{J}/\Delta. \tag{A2}$$

The sixteen eigenvalues and eigenfunctions for $\mathcal{H}_{20}$ follow, where $\mathfrak{N}_i$ in each case is the normalizing factor.

$$\nu_1/\Delta,\ \nu_2/\Delta=1+2\langle\Gamma_{4c}\mid J_z\mid\Gamma_{4c}\rangle^2A\mp\tfrac{1}{2}(4+16\langle\Gamma_{4c}\mid J_z\mid\Gamma_{4c}\rangle^2A+[16\langle\Gamma_{4c}\mid J_z\mid\Gamma_{4c}\rangle^4+48\langle\Gamma_{4b}\mid J_z\mid\Gamma_1\rangle^4]A^2)^{1/2}. \tag{A3a}$$

Here and below, the $-$ sign in front of the square root gives the first eigenvalue on the left-hand side; the $+$ sign gives the second eigenvalue.

$$\mid\alpha_1\rangle=\mathfrak{N}_1\mid\Gamma_1,\ \Gamma_1\rangle-(\mathfrak{N}_1\nu_1/2\sqrt{3}\langle\Gamma_{4b}\mid J_z\mid\Gamma_1\rangle^2A)\tfrac{1}{3}\sqrt{3}(\mid\Gamma_{4b},\ \Gamma_{4b}\rangle-\mid\Gamma_{4a},\ \Gamma_{4c}\rangle-\mid\Gamma_{4c},\ \Gamma_{4a}\rangle), \tag{A3b}$$

$$\mid\alpha_2\rangle=(\mathfrak{N}_1\nu_1/2\sqrt{3}\langle\Gamma_{4b}\mid J_z\mid\Gamma_1\rangle^2A)\mid\Gamma_1,\ \Gamma_1\rangle+(\mathfrak{N}_1/\sqrt{3})(\mid\Gamma_{4b},\ \Gamma_{4b}\rangle-\mid\Gamma_{4a},\ \Gamma_{4c}\rangle-\mid\Gamma_{4c},\ \Gamma_{4a}\rangle), \tag{A3c}$$

$$\nu_3/\Delta=2-2A\langle\Gamma_{4c}\mid J_z\mid\Gamma_{4c}\rangle^2, \tag{A4a}$$

$$\mid\alpha_3\rangle=\tfrac{1}{6}\sqrt{6}(2\mid\Gamma_{4b},\ \Gamma_{4b}\rangle+\mid\Gamma_{4a},\ \Gamma_{4c}\rangle+\mid\Gamma_{4c},\ \Gamma_{4a}\rangle), \tag{A4b}$$

$$\nu_4/\Delta=1-2A\langle\Gamma_{4b}\mid J_z\mid\Gamma_1\rangle^2, \tag{A5a}$$

$$\mid\alpha_4\rangle=\tfrac{1}{2}\sqrt{2}(\mid\Gamma_1,\ \Gamma_{4b}\rangle+\mid\Gamma_{4b},\ \Gamma_1\rangle), \tag{A5b}$$

$$\nu_5/\Delta,\ \nu_6/\Delta=\tfrac{3}{2}+(\langle\Gamma_{4b}\mid J_z\mid\Gamma_1\rangle^2+\langle\Gamma_{4c}\mid J_z\mid\Gamma_{4c}\rangle^2)A\mp\tfrac{1}{2}[1+4A(-\langle\Gamma_{4b}\mid J_z\mid\Gamma_1\rangle^2+\langle\Gamma_{4c}\mid J_z\mid\Gamma_{4c}\rangle^2)$$
$$+4A^2(\langle\Gamma_{4b}\mid J_z\mid\Gamma_1\rangle^4+\langle\Gamma_{4c}\mid J_z\mid\Gamma_{4c}\rangle^4+14\langle\Gamma_{4b}\mid J_z\mid\Gamma_1\rangle^2\langle\Gamma_{4c}\mid J_z\mid\Gamma_{4c}\rangle^2)]^{1/2}, \tag{A6a}$$

$$\mid\alpha_5\rangle=\mathfrak{N}_5\tfrac{1}{2}\sqrt{2}(\mid\Gamma_1,\ \Gamma_{4b}\rangle-\mid\Gamma_{4b},\ \Gamma_1\rangle)+\mathfrak{N}_5\frac{(1+2\langle\Gamma_{4b}\mid J_z\mid\Gamma_1\rangle^2A-\nu_5)}{2\langle\Gamma_{4a}\mid J^-\mid\Gamma_1\rangle\langle\Gamma_{4c}\mid J^+\mid\Gamma_{4b}\rangle A}\tfrac{1}{2}\sqrt{2}(\mid\Gamma_{4a},\ \Gamma_{4c}\rangle-\mid\Gamma_{4c},\ \Gamma_{4a}\rangle), \tag{A6b}$$

$$|\alpha_6\rangle=\frac{\mathfrak{N}_5(1+2\langle\Gamma_{4b}|J_z|\Gamma_1\rangle^2A-\nu_5)}{2\langle\Gamma_{4a}|J^-|\Gamma_1\rangle\langle\Gamma_{4c}|J^+|\Gamma_{4b}\rangle A}\frac{1}{\sqrt{2}}(|\Gamma_1,\Gamma_{4b}\rangle-|\Gamma_{4b},\Gamma_1\rangle)-\mathfrak{N}_5\tfrac{1}{2}\sqrt{2}(|\Gamma_{4a},\Gamma_{4c}\rangle-|\Gamma_{4c},\Gamma_{4a}\rangle), \quad \text{(A6c)}$$

$$\nu_7/\Delta=\nu_4/\Delta, \quad \text{(A7a)}$$

$$|\alpha_7\rangle=\tfrac{1}{2}\sqrt{2}(|\Gamma_1,\Gamma_{4a}\rangle+|\Gamma_{4a},\Gamma_1\rangle), \quad \text{(A7b)}$$

$$\nu_8/\Delta=\nu_3/\Delta, \quad \text{(A8a)}$$

$$|\alpha_8\rangle=\tfrac{1}{2}\sqrt{2}(|\Gamma_{4b},\Gamma_{4a}\rangle+|\Gamma_{4a},\Gamma_{4b}\rangle), \quad \text{(A8b)}$$

$$\nu_9/\Delta=\nu_5/\Delta, \qquad \nu_{10}/\Delta=\nu_6/\Delta, \quad \text{(A9a)}$$

$$|\alpha_9\rangle=\mathfrak{N}_5\tfrac{1}{2}\sqrt{2}(|\Gamma_1,\Gamma_{4a}\rangle-|\Gamma_{4a},\Gamma_1\rangle)-\frac{\mathfrak{N}_5(1+2\langle\Gamma_{4b}|J_z|\Gamma_1\rangle^2A-\nu_5)}{2\langle\Gamma_{4a}|J^-|\Gamma_1\rangle\langle\Gamma_{4c}|J^+|\Gamma_{4b}\rangle A}\tfrac{1}{2}\sqrt{2}(|\Gamma_{4b},\Gamma_{4a}\rangle-|\Gamma_{4a},\Gamma_{4b}\rangle), \quad \text{(A9b)}$$

$$|\alpha_{10}\rangle=\frac{\mathfrak{N}_5(1+2\langle\Gamma_{4b}|J_z|\Gamma_1\rangle^2A-\nu_5)}{2\langle\Gamma_{4a}|J^-|\Gamma_1\rangle\langle\Gamma_{4c}|J^+|\Gamma_{4b}\rangle A}\tfrac{1}{2}\sqrt{2}(|\Gamma_1,\Gamma_{4a}\rangle-|\Gamma_{4a},\Gamma_1\rangle)+\mathfrak{N}_5\tfrac{1}{2}\sqrt{2}(|\Gamma_{4b},\Gamma_{4a}\rangle-|\Gamma_{4a},\Gamma_{4b}\rangle), \quad \text{(A9c)}$$

$$\nu_{11}/\Delta=\nu_3/\Delta, \quad \text{(A10a)}$$

$$|\alpha_{11}\rangle=|\Gamma_{4c},\Gamma_{4c}\rangle, \quad \text{(A10b)}$$

$$\nu_{12}/\Delta=\nu_4/\Delta, \quad \text{(A11a)}$$

$$|\alpha_{12}\rangle=\tfrac{1}{2}\sqrt{2}(|\Gamma_1,\Gamma_{4c}\rangle+|\Gamma_{4c},\Gamma_1\rangle), \quad \text{(A11b)}$$

$$\nu_{13}/\Delta=\nu_3/\Delta, \quad \text{(A12a)}$$

$$|\alpha_{13}\rangle=\tfrac{1}{2}\sqrt{2}(|\Gamma_{4b},\Gamma_{4c}\rangle+|\Gamma_{4c},\Gamma_{4b}\rangle), \quad \text{(A12b)}$$

$$\nu_{14}/\Delta=\nu_5/\Delta, \qquad \nu_{15}/\Delta=\nu_6/\Delta \quad \text{(A13a)}$$

$$|\alpha_{14}\rangle=\mathfrak{N}_5\tfrac{1}{2}\sqrt{2}(|\Gamma_1,\Gamma_{4c}\rangle-|\Gamma_{4c},\Gamma_1\rangle)+\frac{\mathfrak{N}_5(1+2\langle\Gamma_{4b}|J_z|\Gamma_1\rangle^2A-\nu_5)}{2\langle\Gamma_{4a}|J^-|\Gamma_1\rangle\langle\Gamma_{4c}|J^+|\Gamma_{4b}\rangle A}\tfrac{1}{2}\sqrt{2}(|\Gamma_{4b},\Gamma_{4c}\rangle-|\Gamma_{4c},\Gamma_{4b}\rangle), \quad \text{(A13b)}$$

$$|\alpha_{15}\rangle=\frac{\mathfrak{N}_5(1+2\langle\Gamma_{4b}|J_z|\Gamma_1\rangle^2A-\nu_5)}{2\langle\Gamma_{4a}|J^-|\Gamma_1\rangle\langle\Gamma_{4c}|J^+|\Gamma_{4b}\rangle A}\tfrac{1}{2}\sqrt{2}(|\Gamma_1,\Gamma_{4c}\rangle-|\Gamma_{4c},\Gamma_1\rangle)-\mathfrak{N}_5\tfrac{1}{2}\sqrt{2}(|\Gamma_{4b},\Gamma_{4c}\rangle-|\Gamma_{4c},\Gamma_{4b}\rangle), \quad \text{(A13c)}$$

$$\nu_{16}/\Delta=\nu_3/\Delta, \quad \text{(A14a)}$$

$$|\alpha_{16}\rangle=|\Gamma_{4a},\Gamma_{4a}\rangle. \quad \text{(A14b)}$$